Modeling wildfire spread in wildland-industrial interfaces using dynamic Bayesian network

Khakzad, N.

DOI
10.1016/j.ress.2019.04.006

Publication date
2019

Document Version
Accepted author manuscript

Published in
Reliability Engineering & System Safety

Modeling wildfire spread in wildland-industrial interfaces using dynamic Bayesian network

Nima Khakzad

Faculty of Technology, Policy, and Management, Delft University of Technology, The Netherlands

Email: n.khakzadrostami@tudelft.nl

Address: Jaffalaan 5, Delft 2628BX, The Netherlands

Abstract

Global warming and the subsequent increase in the frequency and severity of wildfires demand for specialized risk assessment and management methodologies to cope with the ever-increasing risk of wildfires in wildland-industrial interfaces (WIIs). Wildfires can jeopardize the safety and integrity of industrial plants, and trigger secondary fires and explosions especially in the case of process plants where large inventory of combustible and flammable substances is present. In the present study, modeling the WII as a two dimensional lattice, we have developed an innovative methodology for risk assessment of wildfire in WIIs by combining the dynamic Bayesian network and wildfire behavior prediction models. The developed methodology models the spatial and temporal spread of fire in WIIs, based on the most probable path of fire, both in the wildland and in the industrial area.

Keywords: Wildland-industrial interface; Wildfire; NaTech accident; Dynamic Bayesian network; Fire's most probable path; Domino effect.

1. Introduction

Every year, wildfires burn between 300 to 600 million hectares of land globally, with an annual average of 297 fatalities between 2008 and 2015 [1]. Wildfires are classified as hydro-geological events which are bound to increase due to the combined effects of climate change and human development. Regarding the climate change, every degree in global warming may result in a 12% increase in the lightning [2], as one of the main causes of wildfires, while to compensate for the increase in the risk of consequent wildfires 15% more precipitation would be required [3]. With the increase in human development and activities in wildlands, the likelihood of human-caused wildfires has increased; this is because, unlike most natural disasters, four out of five wildfires (80%) are started by people [4]. In the Mediterranean countries, human activities account for more than 90% of wildfires [5]. Aside from the role of human in causing wildfires, the ever-increasing development in urban and industrial areas has increased the wildland-human interfaces, exposing the assets to a greater risk of damage in the event of wildfires.

Wildland-human interfaces can be in the form of wildland-urban interfaces (WUIs), wildland- industrial interfaces (WIIs), and wildland-infrastructure interfaces [6]. WII is an area where, for instance, oil & gas facilities or other industrial plants meet with or are located within wildland vegetation. Most previous works and attempts in modeling and risk assessment of wildfires in wildland-human interfaces have been devoted to wildlands or WUIs [7-10] with a very few studies to WIIs [11,12].

Modeling and risk assessment of fires in WIIs are important because, in addition to the potential of damage to industrial facilities, the loss of revenue due to the facilities' operations shutdown (for safety concerns or repair and replacement of damaged units) could be substantial. For instance, in May 2015, wildfires in the province of Alberta, Canada, spread to the oilsands areas, causing two major petroleum companies, Canadian Natural and Cenovus Energy, to shut down their 80,000 and 135,000-barrel-a-day operations, respectively [13]. In May 2016, wildfires burned part of Fort McMurray, Alberta, Canada, and moved towards oilsands plants north of the city (Figure 1), causing a 40% drop in the oil production due to the shutdown of oilsands facilities nearby [14].

Wildfires in WIIs can result in catastrophic consequences particularly in the case of oil and gas facilities (refineries, storage plants, etc.). Exposed to the heat of wildfire, storage tanks of flammable and explosive petroleum products such as crude oil, gasoline, diesel, kerosene, and propane can get damaged (through heat convection, radiation, or airborne embers), and help spread the fire to other units and storage tanks – known as a domino effect.

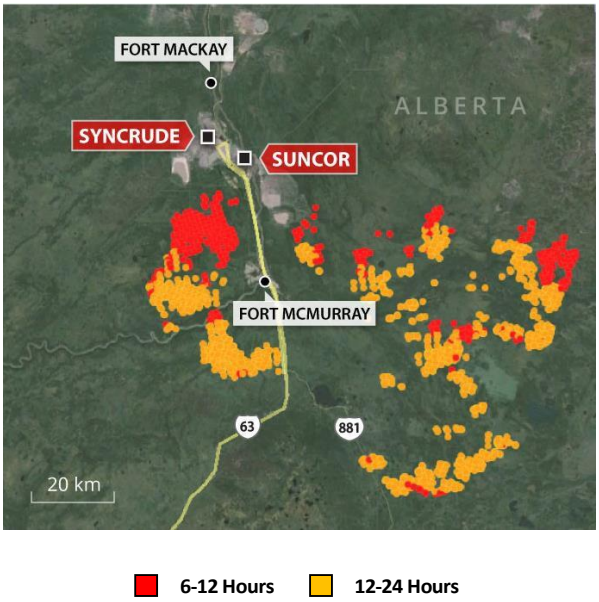

Figure 1. Wildfire in Fort McMurray, Alberta, Canada (as of May 17, 2016), threatening major oilsands operation facilities owned by Suncor and Syncrude. Red and yellow spots denote the fire spread 6-12 hours and 12-24 hours, respectively, after the onset of fire [15].

In order to protect oil and gas facilities from wildfires (and also protect the wildlands from potential ignitions at the facilities), there must be buffer zones, usually in the form of vegetation-free ground, between the facilities and forest vegetation. In the absence of specialized fire spread modeling and risk assessment methodologies in WIIs, such buffer zones are usually determined based on rule of thumb and approximate analysis [16]. However, recent research has demonstrated that these buffer zones are not sufficient in most cases [17].

The present study is aimed at developing a methodology by integrating dynamic Bayesian network (DBN) and fire behavior prediction models to simulate the spread of wildfires (the most probable path) in WIIs. In order to predict the fire behavior and characteristics such as the rate of spread and intensity, the Canadian fire Behavior Prediction (FBP) system – an online public wildfire information system [18] – is used. A review of wildfire modeling and risk assessment techniques is given in Section 2. DBN and its application to industrial fire spread modeling [19] are briefly revisited in Section 3. In Section 4, the DBN is adapted and integrated with the FBP system to model the spread and assess the impact of wildfires in WIIs. The conclusions are presented in Section 5.

2. Wildfire risk assessment

Wildfire hazard is usually expressed using the fire behavior [1], the main constituting factors of which are the rate of spread and the fire head intensity. Fire behavior models take into account the weather and fuel conditions and landscape topography to calculate the rate of spread, the amount of consumed fuel, the overall shape of the fire perimeter, the rate of energy release, the mode of propagation (surface fire, crown fire, or intermittent), and the geometry of the flame [20]. Accordingly, the risk of wildfire-induced damage to human, assets, and the environment can be defined based on the fire likelihood, fire behavior (rate of spread and intensity), and the impact of fire on the target [9,21]. In other words, in a WII with K targets, the risk of wildfire can be expressed as:

$$\sum \quad \sum \quad \sum \qquad ( ) (|) (|) \tag{1}$$

where ( ) is the probability of ignition in the cell i of the wildland; N is the total number of ignitable cells (green cells) depending on the resolution of the representative lattice; (|) is the probability of ignition evolving as a wildfire with a given intensity; M is the number of possible fire intensity; (|) is the response function (vulnerability) of target k to a wildfire of certain intensity.

2.1. Ignition probability

The probability of ignition P(I), which can reasonably be taken as the probability of small wildfires (≤ 10 hectare), is usually modeled statistically using fire occurrence data [22]. Weather conditions such as temperature, relative humidity, and wind speed are the main factors in the estimation of P(I) (or small fires). The vegetation moisture content also plays a key role in both the initiation of fire (the ignition) and the continuation and spread of it [23].

Based on the foregoing spatial and temporal factors, several statistical relationships have been developed for the prediction of P(I) [7,24,25]. For instance, Preisler et al. [7] used a logistic regression technique to predict the probability of small fires (fire in an area of 0.04 ha), based on parameters such as burning index, fire potential index, drought index, thousand-hour fuel moisture, wind speed, relative humidity, dry bulb temperature, day of the year, and elevation.

Considering the lightning as one of the main triggers of wildfires, studies have been devoted to the estimation of lightning-induced ignitions [26,27]. Regarding the human-induced ignition as the most common type of ignition, Lawson et al. [28] developed the Wildfire Ignition Probability Predictor

(WIPP) model based on the wind speed and the fuel moisture content to predict the P(I) in the forests of British Columbia, Canada.

2.2. Spread probability

For large wildfires (> 10 hectare), in addition to the P(I), the spread probability P(WF|I) – also known as the burn probability – would be needed to estimate the probability and assess the risk of wildfire [22]. One way to estimate the spread probability is to consider many thousands of ignitions in the wildland, and simulate their potentiality of growing as a wildfire using fire spread models to find the relative frequency of fires which would spread and threaten the targets of interest [9,29]. Nevertheless, most wildfires that cause significant damage to the assets start from the ignitions close to wildland-human interfaces where the likelihood of human-induced ignitions are high [30]. That being said, when assessing the impacts of wildfires on wildland-human interfaces, the distant ignitions can reasonably be screened out from the risk assessment.

Many fundamental models have been developed for predicting the behavior of fire in wildland fuels, including the surface fires [31, 32], crown fires [33-35], and the spread of fire by means of airborne ambers and fire brands (known as spotting) [36,37].

Modeling the wildland as a grid or graph, a number of deterministic and probabilistic methodologies has been developed to model fire spread from cell to cell (in the case of grids) or node to node (in the case of graphs). Some of deterministic fire spread models include the turbulent forest fire model based on the distribution and dissipation of energy [38-40], the shortest travel time [41-43], the shortest path algorithms [44], fuzzy cellular automata [45], and the integration of cellular automata and genetic algorithm [46]. Some of probabilistic fire spread models include the works based on continuous-time Markov chain [47], stochastic shortest path [48], and the most probable path [49].

Likewise, a number of wildfire spread and behavior simulation models have been developed such as BEHAVE [50], the National Bushfire Model [51], and FARSITE [52], mainly based on the fundamental fire behavior models. A review of wildfire simulators has been given in Papadopoulos and Pavlidou [53], pointing out FARSITE as the most precise fire propagation simulator.

Similarly, a number of wildfire simulation software and applications have been generated, including the Canadian Fire Behavior Prediction System[1] [18], NEXUS[2] [54], FlamMap[3] [55], BehavePlus[4] [56],

[1] http://cwfis.cfs.nrcan.gc.ca/home
[2] http://pyrologix.com/downloads/#software
[3] https://www.fs.fed.us/rmrs/tools/flammap
[4] https://www.frames.gov/partner-sites/behaveplus/home

FOFEM[5] [57], and FSPro[6] [58], and FARSITE[7] [52]. Effective applications of the most of these simulators require adequate knowledge and skill of Geographic Information System (GIS) and wildland fuel modeling techniques [1] as well as detailed spatial information on topography, fuels, and weather conditions, which does not exist for many wildland-human interfaces.

2.3. Fire intensity

2.3.1. Fire head intensity

To assess the response function of targets exposed to the fire, estimating the intensity of the fire both at the fire head and at the targets, which may not be in direct contact with the fire head, would be required. Fire head intensity (q) is the rate of energy release per unit length of the fire head (kW/m), regardless of the fire's depth. Having the rate of spread ( ) and the amount and the type of the consumed fuel, the fire head intensity can be calculated [31,59]. Using the relationship developed by Byram [31], q can be calculated as:

(—) (2)

where q (kW/m) is the fire head intensity; ρ (kJ/kg) is the fuel low heat of combustion, that is, the high heat of combustion minus the heat losses from radiation, incomplete combustion, and fuel moisture; is the fuel consumption rate in the fire head (kg/m^2), and (m/min) is the rate of fire spread. Without having the rate of spread and the fuel's characteristics, the fire head intensity can still be calculated if the flame length, L(m) is known [31]:

(3)

The fire's different zones such as the fire head and flanks as well as the flame's characteristics such as its length (L), height (H), depth (D), and angle (α) are depicted in Figure 2. In the case of crown fires, one-half of the mean canopy height should also be added to L [31]. A review of relationships to calculate the fire intensity based on the fire length can be found in [60].

[5] https://www.fs.usda.gov/ccrc/tools/fofem
[6] https://wfdss.usgs.gov/wfdss_help/WFDSSHelp_request_acct.html
[7] https://www.firelab.org/document/farsite-software

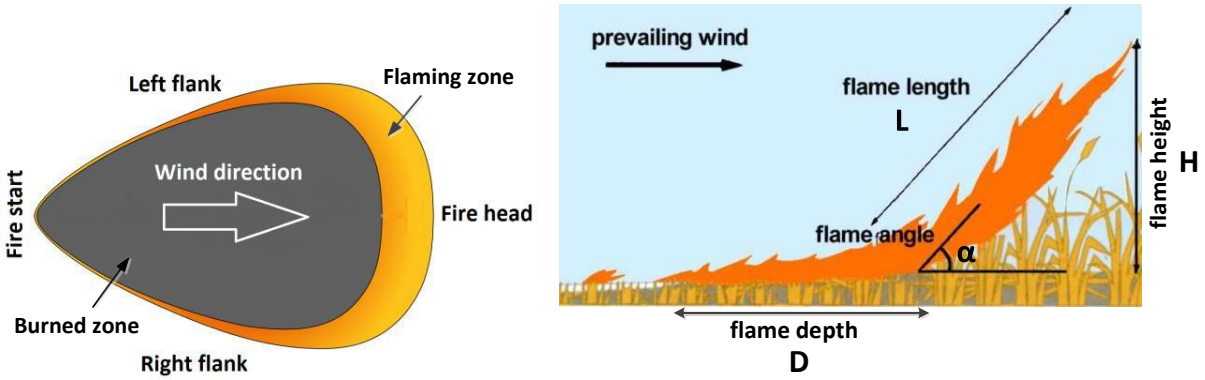

(a) (b)

Figure 2. (a) Fire zones (adapted from Wikipedia). (b) Flame characteristics [61].

Having the flame depth, the head fire intensity can be converted to area-fire or reaction intensity Q (kW/m^2) [62]:

– (4)

2.3.2. Fire intensity received by a target

Wildfire spread in forest vegetation is governed by heat transfer and mass transfer rules in the form of convection, radiation, and spotting [49]. To protect industrial plants and facilities from the impact of wildfire (and also to protect the forest vegetation from industrial fires), there should be a buffer zone or safety distance in the form of vegetation-free ground between facilities and the forest vegetation in the WIIs [16]. However, numerical simulations of storage tanks exposed to wildfire has demonstrated that in most cases such safety distances would not be adequate to sufficiently lower the risk of damage caused by radiant heat [17].

To account for the risk of damage due to the wildfire radiant heat, the fire's intensity received by target facilities (or units) at variable distances from the fire head (or flanks) would be required. Having the fire intensity at the targets along with the type (e.g., atmospheric storage tanks) and characteristics of the target vessels and equipment (e.g., the type of material, wall thickness), the probability of damage can be assessed using, for instance, dose-response or fragility relationships [63, 64]. Considering the flame as a solid body [17, 65, 66], the fire reaction intensity at a distance of r from the flame, , can be calculated using the solid flame model [67] as:

(5)

where F_{view} is the view factor, i.e., the fraction of the heat radiation received by a target [68], and is the atmospheric transmissivity ($0 \leq \leq 1$) to account for the fraction of the radiant heat diminished due to the distance and the atmospheric humidity and carbon dioxide.

3. Industrial fire spread modeling using Bayesian network

3.1. Dynamic Bayesian network

A Bayesian network [69] is a probabilistic model BN= (G, θ) for reasoning under uncertainty, where G is the model structure in the form of a directed acyclic graph, and θ is the model parameters in the form of conditional probabilities. G presents the conditional dependencies among the nodes (random variables) of the graph by means of directed arcs – drawn from the parent nodes to the child nodes – while the conditional probabilities assigned to the child nodes determine the type of the dependencies. The nodes with no parents (known as root nodes) are assigned marginal probabilities. BN takes advantage of the d-separation rule to simplify the joint probability distribution of its nodes. Considering the BN in Figure 3, the d-separation rule can be expressed as:

- in a serial connection as X1, X2, and X5, if the state of X2 is known, X1 and X5 become conditionally independent: P(X5|X1, X2) = P(X5|X2)
- in a divergent connection as X2, X4, and X5, if the state of X2 is known, X4 and X5 become conditionally independent: P(X5|X2, X4) = P(X5|X2)
- in a convergent connection as X1, X2, and X3, if the state of X2 is unknown, X1 and X3 become independent: P(X1|X3) = P(X1)

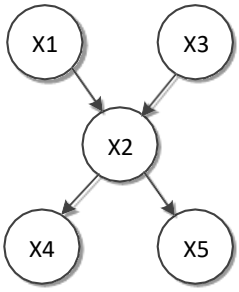

Figure 3. A typical Bayesian network. X1 and X3 are root nodes. X1 and X3 are the parents of X2 and ancestors of X4 and X5. X2 is the child of X1 and X3 while X4 and X5 are the descendants of X1 and X3. X1, X2, X3, and X4 are non-descendants of X5.

The d-separation rule can be manifested as the Markovian property: Given its parents, a node becomes conditionally independent of all its non-descendants. For instance, P(X5|X1, X2) = P(X5|X2) and P(X5|X2, X4) = P(X5|X2). Satisfying the Markovian property, the joint probability distribution of the variables in a BN can be factorized as the product of the nodes' conditional probabilities given their immediate parents. Considering the BN in Figure 3: P(X1, X2, X3, X4, X5) = P(X1) P(X3) P(X2|X1, X3) P(X4|X2) P(X5|X2).

Having the joint probability distribution of the variables, the marginal probability of any of the nodes can be calculated using a number of inference algorithms such as bucket elimination (a.k.a variable elimination) [70], junction tree [71, 72], belief propagation (a.k.a sum-product message passing) [73], and Monte Carlo Markov Chain analysis [74].

A BN can be extended to a dynamic Bayesian network (DBN) so that the dynamic aspects and temporal uncertainties arising from the sequence of failures (or events) or temporal changes (aging, growth, degradation, etc.) can be considered in the modeling. To form a DBN, a BN (as a snapshot of the system) is usually replicated in time slices over a specific time period.

Figure 4(a) displays a two-slice DBN where the nodes of the more recent time slice are denoted with a prime symbol and a darker color. In Figure 4(a), the arc from X3 to itself but in another time slice, X3', implies the temporal evolution of X3 (e.g., weakening due to fatigue) while the arc from X5 to X2' may indicate either a reciprocal cause-effect relationship (X2 → X5 → X2) or uncertainty about the sequence of failures (X2 → X5 or X5 → X2?), neither of which possible to be modeled in BN.

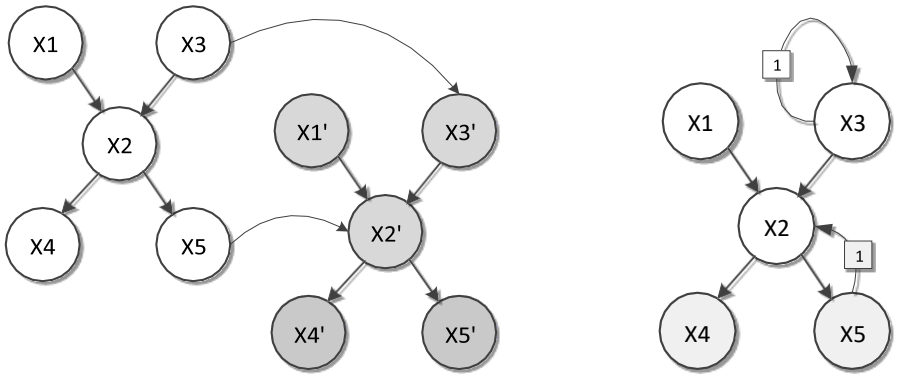

Figure 4. (a) A two-slice DBN in extended form. (b) The same DBN in abstract form. The numbers attached to the arcs denote the number of time slices used for temporal dependencies.

3.2. Fire spread in industrial plants

Khakzad et al. [75] developed a methodology based on BN for modeling the spread of fire (domino effect) in process plants, presenting the process units as the nodes and the possibility of fire spread between the adjacent nodes (from burning units to the exposed units) as the directed arcs of the BN. In their approach, the conditional probabilities assigned to the exposed units were determined using dose-response relationships (probit functions) developed for estimating the damage probability of process units exposed to fire [63].

Modeling the fire spread as a BN, given a primary fire, exposed units with the highest marginal probability were chosen as the secondary units involved in the fire spread. Following the same approach, the tertiary units can be identified, and so on. Figure 5 displays a tank terminal and the BN developed for modeling the fire spread in the terminal given a primary fire at T2 (e.g., a gasoline tank).

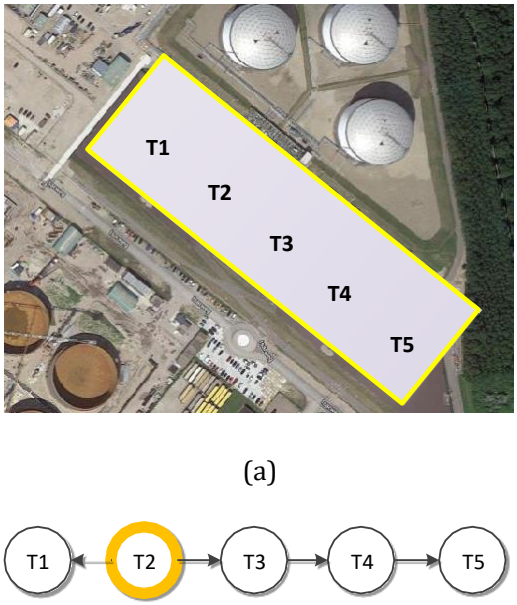

Figure 5. (a) A tank terminal. (b) Modeling of fire spread as a BN given fire at T2.

The application of BN to fire spread modeling does not capture the uncertainty arising from different possible fire spread paths. In the tank terminal of Figure 5, for instance, if there were two simultaneous primary fires at T2 and T5, two different BNs could be developed for fire spread

modeling, as shown in Figures 6(a) and (b). As mentioned in the previous section, DBN can be used to account for the uncertainty arising from the analyst's doubt about the sequence of failures (here, the sequence of fires). For this purpose, the DBN methodology developed by Khakzad [19] can be applied, as depicted in Figure 6(c).

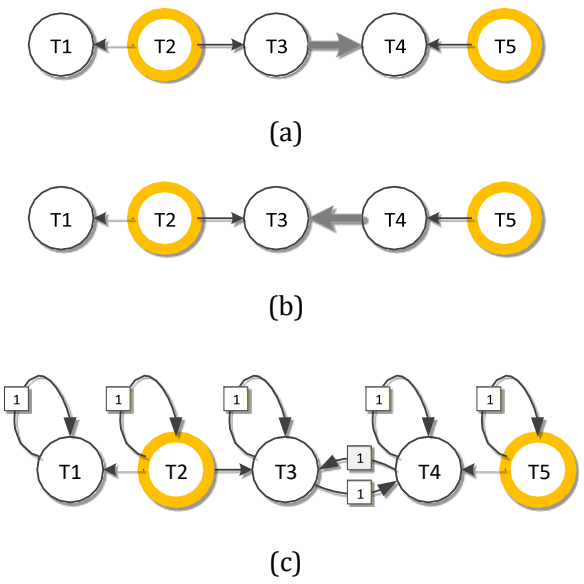

Figure 6. BNs for modeling possible fire spread given primary fires at T2 and T5 where (a) T3 may catch fire before T4, and (b) T4 may catch fire before T3. (c) Fire spread modeling as a DBN to account for uncertain fire spread paths in panels a and b.

4. Wildfire spread modeling using Bayesian network

4.1 Methodology

The DBN methodology developed for modeling industrial fire spread can be adapted to modeling wildfire spread in WIIs via the following steps:

(i) the WII of interest is first modeled as a 2D lattice;

(ii) the lattice is modeled using a DBN. Each cell of the lattice is presented a node of the DBN. The words "cell" and "node" are thus used interchangeably in the development of the methodology;

(iii) given ignition in an arbitrary cell (provided that the cell is not a bare land), a fire behavior model is used to determine the fire spread rate and intensity;

(iv) fire spread rate and intensity are used to estimate the fire spread probabilities between the cells;

(v) quantifying the DBN using the spread (conditional) probabilities, the most probable path of fire spread is determined.

As discussed in Section 2.2, similar approaches have been adopted in the previous studies [41,47,49]. For instance, by modeling the wildland as a 2D rectangular lattice and by overlaying spatial data of terrain, fuel, and wind, Finney [41] employed fire behavior models such as BEHAVE [50] and FARSITE [52] to model fire spread based on the minimum travel time.

In order to make the discussion more concrete, consider a WII in Figure 7(a) which has been modeled as a lattice consisting of 49 cells of 200m × 200m, of which cells 32 and 33 being occupied by an oil terminal, consisting of five gasoline storage tanks as shown in Figure 7(b). To account for the heterogeneity of the forest vegetation, 20% of the wildland (about 9 out of 47 remaining cells) has been considered as fuel-free (bare land), shown as hatched cells in Figure 7. Considering a uniform distribution for lightning-induced ignition over the landscape [76], fire may start with a certain probability P(I) at any cell with forest vegetation (e.g., cell 23).

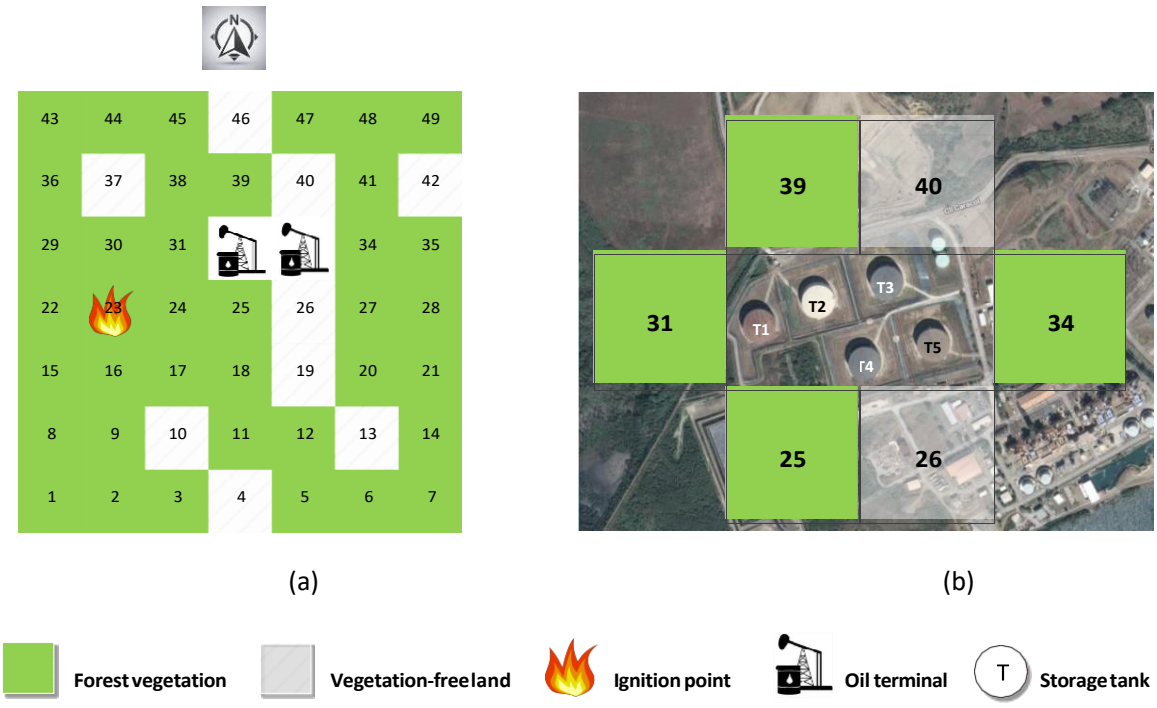

Figure 7. (a) Modeling the wildland-industrial interface as a lattice. Green cells are those with forest vegetation. The hatched cells are vegetation-free land. Cell 23 is where the ignition occurs. Cells 32

and 33 are occupied by an oil terminal. (b) Layout of the oil terminal, consisting of five storage tanks T1-T5. The cells have been numbered from 1 to 49 only for the sake of modeling.

Choosing cell 23 from the green cells, i.e., those with forest vegetation, as the ignition cell via uniform sampling, the potential paths for fire spread are modeled as the DBN in Figure 8, where every cell of the lattice, except cells 32 and 33, has been modeled as a corresponding node. Instead of cells 32 and 33, the five storage tanks T1-T5 have been modeled as separate nodes (highlighted with color blue).

It should be noted that although the fuel-free nodes (highlighted with color grey) do not contribute to the fire spread, they have been included in the model so that the developed DBN would be applicable to different scenarios and forest vegetation densities. However, their states have been set to "no-fuel" to neutralize their role in the fire spread modeling. Cell 23, where the ignition starts, have been highlighted with color yellow. Two more assumptions have been made in the development of the DBN: (i) only the spread of fire from the wildland to the industrial plant is considered, ruling out the possibility of a burning tank igniting forest vegetation in the adjacent cells (that is why there is no arc from T1-T5 to the wildland nodes); (ii) fire in a burning cell can spread to other green cells in its van Neumann neighborhood.

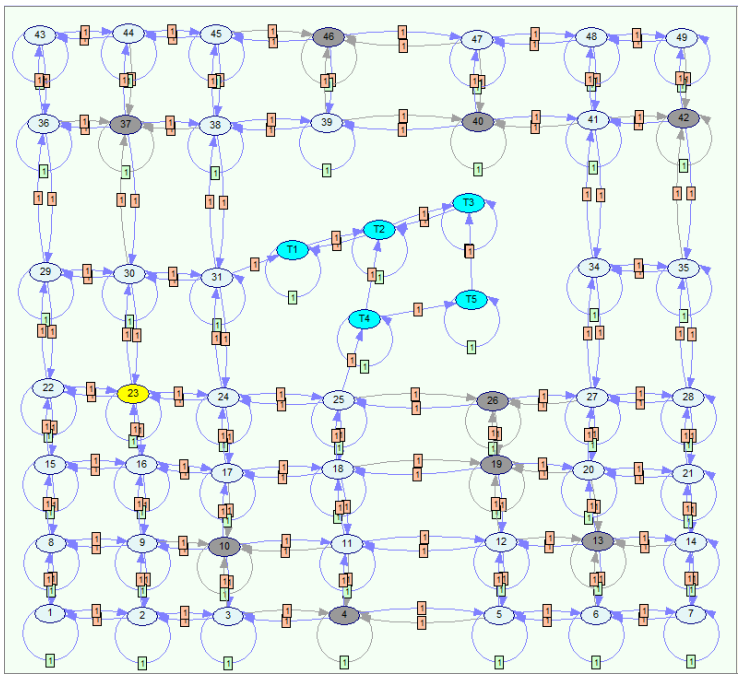

Forest vegetation

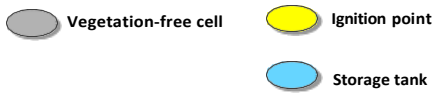

Figure 8. DBN for modeling the fire spread in WII. The storage tanks T1-T5 are denoted by color blue, fuel-free nodes by color grey, and the ignition node by color yellow.

Two main types of neighborhood, that is, Moore neighborhood and van Neumann neighborhood, have been depicted in (Figure 9).

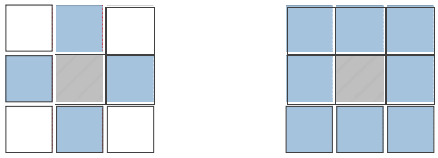

(a) (b)

Figure 9. (a) van Neumann neighborhood. (b) Moore neighborhood.

To quantify the DBN and model the fire growth in the WII, the fire spread probabilities between the nodes are required. Assuming that the forest vegetation would certainly catch fire in contact with the flames [49], the probability of fire spread among the forest vegetation cells would depend on the direction of wind and the rate of fire spread.

Assuming that the wind direction would be along the length of the cells, the probability of fire spread in the fire head (direction of wind) can be calculated as the probability that in a given time interval (τ) the fire burns along the burning cell (d) and reach the adjacent green cell. In other words, the probability of fire spread would be equal to the probability of the fire's travel time between two cells (t) being less than the given time interval (τ). Since the fire travel time can be calculated as ,the probability of fire spread in the direction of wind during any two sequential time slices (τ) in the DBN can be estimated as ( ). Having the probability density function of the rate of spread ( ), the probability of spread can be calculated as:

( )

– ( ) (–) (–) ∫ ( ) ( ) –

(6)

where (.) is the cumulative density function of .

In the present study, the Fire Behavior Prediction (FBP) System embedded in the Canadian Wildland Fire Information System [18], a public online application, is employed to predict the wind direction, the rate of spread (m/min) and the fire intensity (kW/m) on a daily basis. Given the geographical location of the WII, the information derived from FBP system, in the form of interactive maps, can be overlaid on the representative lattice, as illustrated in Figure 10.

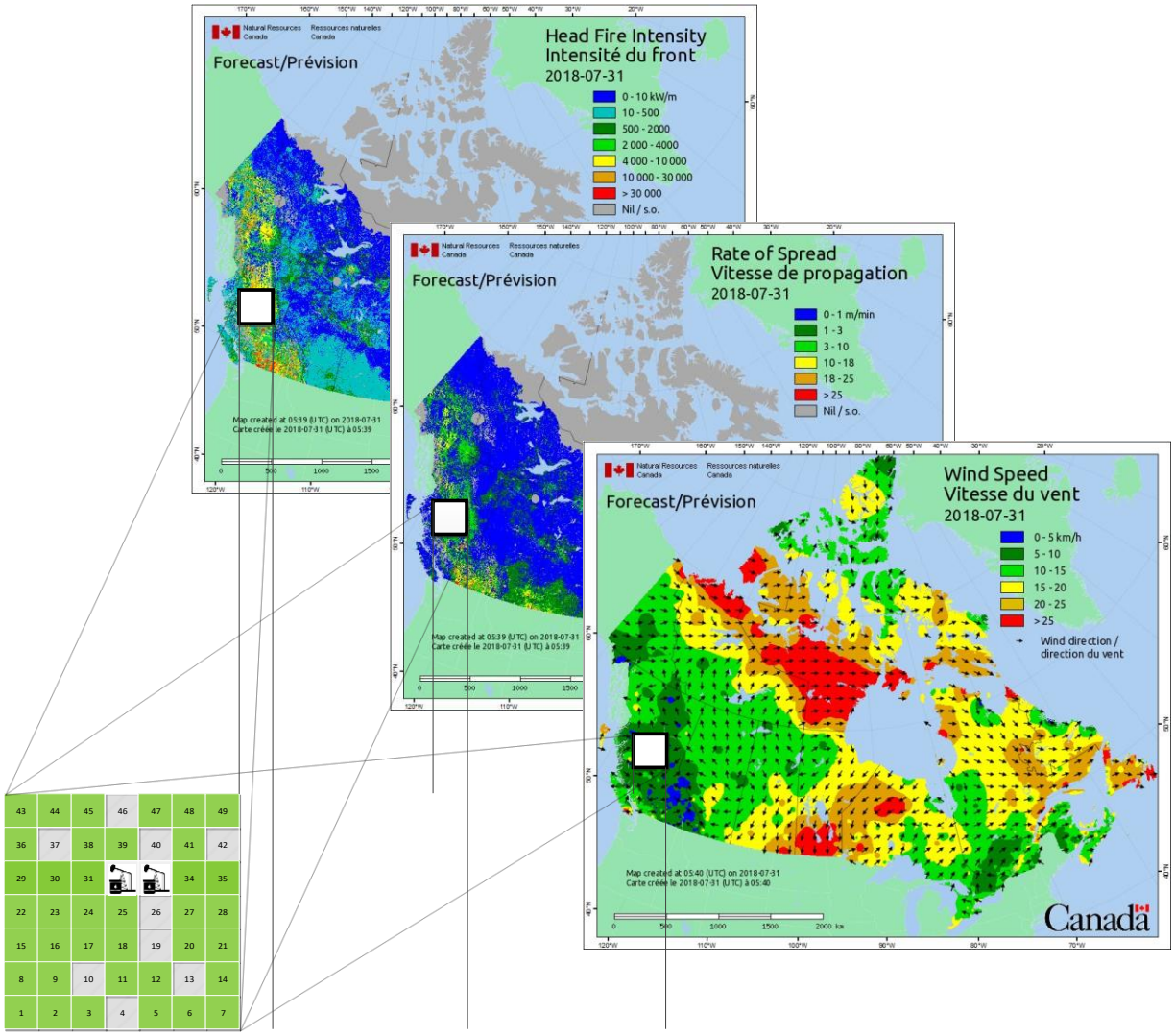

Figure 10. Given the location of the WII, the fire's rate of spread and intensity as well as weather conditions can be determined using the Canadian Forest Fire Behavior System.

4.2. Results

Assuming that wind direction is from south to north, and the rate of spread is a normal variable with a mean value and standard deviation of 15 and 3 m/min, respectively, the probability of fire

spread in the north direction can be calculated about 0.7 using Equation (6) given a simulation time interval of τ = 15 min in the DBN and a cell length of d = 200 m.

The fire spread rate in wildfires can vary several orders of magnitude around its perimeter [77], with the highest rate in the direction of wind and at the fire head. Thus, having the probability of fire spread of 0.7 calculated at the fire head (north direction), the probabilities of spread at the fire's flanks (east and west directions) and rear (south direction) were assumed as 0.4 and 0.1, respectively, for illustrative purposes. Implementing the DBN in GeNIe software [78], the spread of fire through the wildland vegetation can be modeled based on the most probable path of fire spread. The results of four representative time slices are shown in Figure 11.

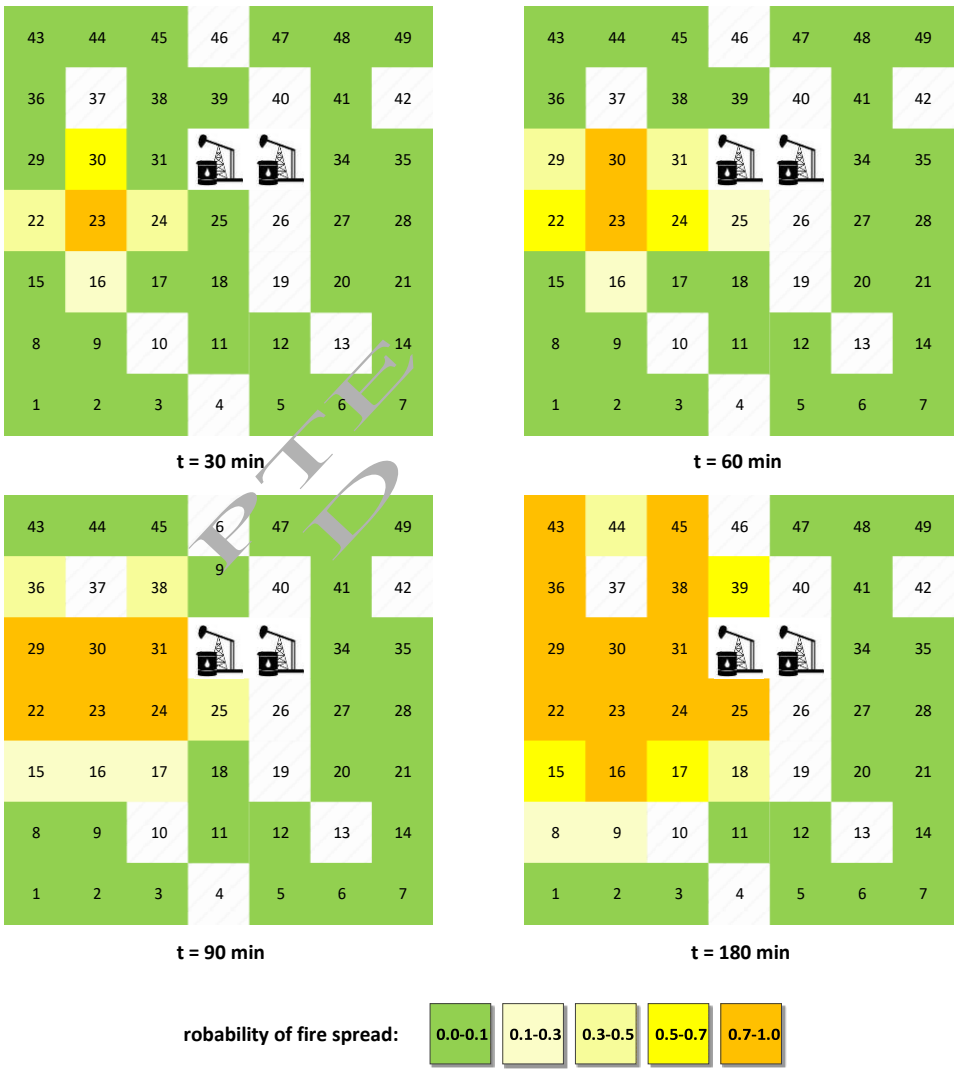

Figure 11. Propagation of wildfire across the wildland within 180 minutes from the start in cell 23 in Figure 7(a). The colors denote the fire spread probabilities varying from the lowest (green: 0.0 ~ 0.1) to the highest (orange: 0.7 ~ 1.0). Probability of zero has been assigned to the hatched area due to the lack of vegetation.

To model the spread of fire from the forest vegetation cells to the storage tanks, the intensity of fire at the cells adjacent to the storage plant would be required. Considering the fire intensity map provided by the Canadian FBP System in Figure 10, an identical intensity of I = 4000 ( ) is considered for the burning cells. Assuming a flame depth of D = 5m, the fire reaction intensity immediately at the wildfire front can be calculated using Equation (4) as Q = 800 ( ). Considering a wind speed of = 5 ( ) and approximately equal distances of T1 and T4 from the centre of the fire as r = 20 m, a view factor of = 0.021 was calculated (see Appendix). Using Equation (5), the magnitude of the heat radiation T1 and T4 receive from the wildfire would be = 16.8 ( ).

If either T1 or T4 catches fire exposed to the heat of wildfire, they can trigger a domino effect inside the oil terminal. To model the fire spread in the oil terminal, the amount of heat radiation an exposed tank may receive from a burning tank is required to calculate the conditional damage probabilities. Having the weather conditions (wind speed: 5 m/s; wind direction: from south to north; relative humidity: 25%) and the type (atmospheric tanks of gasoline) and the size (diameter: 50m, height: 12m, volume: 23,500 m^3) of the storage tanks, the approximate amounts of heat radiation tank Tj receives from a tank fire at Ti were calculated using ALOHA [79], as presented in Table 1.

Table 1. Approximate heat radiation intensity (kW/m^2) tank T_j receives from a tank fire at tank T_i.

T_i	T_j				
	1	2	3	4	5
1		21.1			
2	21.1		21.1	14.6	
3		21.1			14.6
4		31.8			21.1
5			31.8	21.1	

Knowing the amount of radiant heat both from the forest vegetation to the storage tanks (: from cell 31 to T1 and from cell 25 to T4) and from a burning tank to the adjacent tanks (Table 1), the damage probability of tanks can be calculated using probit functions. In the present study, we use probit functions [64] developed for atmospheric process vessels:

( ) ( ) (7)

(—) (8)

( ) (9)

where ttf (s) is the time to failure of an exposed storage tank; Q_r (kW/m^2) is the received heat radiation by the tank from the wildfire or other burning tanks; V (m^3) is the tanks volume; Y is the probit value; Pr is the damage probability of the tank; ϕ(.) is the cumulative density function of standard normal distribution.

It should be noted that the foregoing relationships are valid only if the amount of heat radiation received by an atmospheric storage tank is higher than 15 kW/m^2 [64]. As a result, tank fires at T2 and T3 would not be able to cause damage to T4 and T5, respectively, as the amount of radiant heat that T4 and T5 may receive from T2 and T3 is below the threshold heat (14.6 kW/m^2). Accordingly, in the DBN in Figure 8, there are no arcs from T2 and T3 to T4 and T5. Using the damage probabilities in the DBN, the temporal probabilities of fire spread among the storage tanks have been displayed in Figure 12.

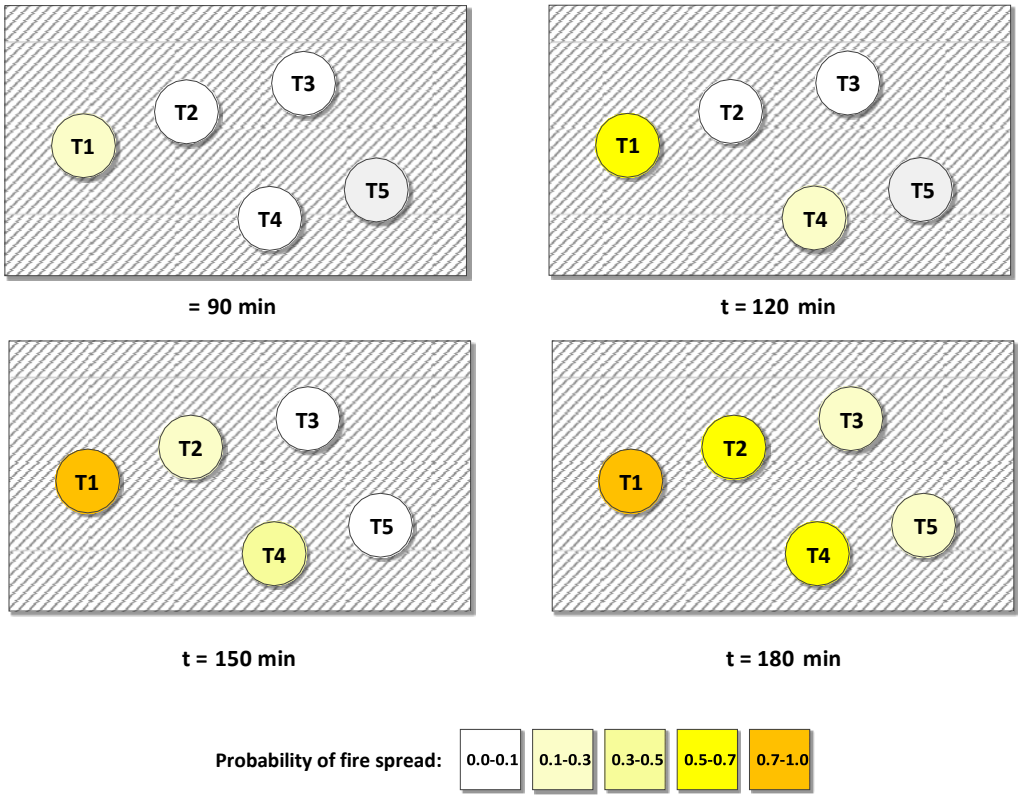

Figure 12. Fire spread probabilities in the storage plant due to wildfire-induced domino effect. The colors denote the fire spread probabilities varying from the lowest (gray: 0.0 ~ 0.1) to the highest (orange: 0.7 ~ 1.0).

4.3. Further remarks

Figure 12 shows that 120 min and 150 min after the onset of fire in cell 23, the probability of fire spread to T1 and T4, respectively, would be credible (more than 50% chance of catching fire). The results shown in Figures 11 and 12, however, should not be taken as the final fire spread probabilities in the WII. As pointed out in Finney [41] and later adopted in Miller et al. [29], Scott et al. [9], and Khakzad et al. [11], the burn probability of a cell – be it a forest vegetation cell or a storage tank – should be estimated as the mean (expected) value of the burn probabilities of the cell by simulating many thousands of random ignitions in the wildland and under different weather and fuel conditions. For instance, considering a constant fuel condition and three prevailing wind conditions in the WII, and knowing that the fire intensity and spread rate are dominant by weather- fuel conditions, the probability of fire spread to T1 can be calculated as:

$$P(\quad) = \sum \quad \sum \quad P(\quad)\,P(\,|\,)\,P(\,|\,) \tag{10}$$

where i = 1, …, 38 is the number of forest vegetation cells in the WII in Figure 7(a), and j = 1, …, 3 is the number of wildfires with different intensity.

In short-term modeling and assessment the risk of wildfires in WIIs, where the fuel and weather circumstances can be considered as constant [41], the possible changes in the fire intensity can be ignored, and thus only the possibility of random ignition points can be taken into account in Equation (10). In other words, to obtain more accurate probabilities in Figures 11 and 12, the modeling should be replicated at least given different ignition points in the lattice of Figure 7(a).

The developed methodology, similarly to other fire spread models which suffer more or less from epistemic and aleatory uncertainties, is subject to two different sources of uncertainty (or simplification): (i) the simplifications made in the fire behavior prediction model, i.e., the Canadian Fire Behavior Prediction System [18], and (ii) the simplifications made in the development of the DBN.

Regarding the former type of simplifications, as argued by Alexander and Cruz [10], the results of most fire simulation models are not accurate because, for instance, they usually assume a continuous, uniform, and homogeneous fuel complex consisting of a single fuel layer (i.e., no distinction between surface and crown fuels). Furthermore, they often overlook the role of spotting or fire whirlwinds in creating multiple fire fronts [49], thus not necessarily resulting in the likeliest path of fire spread. While the short-range spotting may be over burned by the fire head, in long- range spotting the fire brands and ambers can travel in excess of 5 km from the fire line [77] while the fire whirlwinds can travel in excess of 2.5 km from the fire front [80]. Due to the foregoing simplifications, an estimation error threshold of 35% would be acceptable for the predicted rate of spread [10].

Regarding the latter type of simplifications, we made a number of simplifications either for illustrative purposes or for lack of data, which are worth mentioning for the sake of future improvements:

- For a given fuel type, the major fire spread direction is governed by both the wind direction and the terrain slope [41]. Fire, more often than not, moves faster upslope than on a plain terrain as the fire's heat moves upward and preheats the forest vegetation uphill. In the present study, considering the wildland as a 2D lattice, we did not consider the role of slope and assumed that the direction of fire would merely be controlled by the wind direction.
- For each cell of the WII in Figure 7(a), if not a bare land, we considered only two states: burning and not burning, indicating an infinite residence time ( ) for a burning cell. is the

length of time which takes the flame front to pass a given point [62]. It has alternatively been defined as the length of time for which the burning fuel continues to emit heat flux without smoldering or burning out [49]. Using the simplifying assumption of an infinite , as can be seen from Figure 11, a burning cell at t = 30 min would still be burning at t = 180 min with a certain probability, resulting in an overestimation of burn probabilities in the adjacent cells and thus overestimated fire spread probabilities in general. The assumption may be reasonable for short-term (a few hours) modeling and risk assessment of fire spread, but in long-term modeling should be calculated, for instance as –[62], and taken into account in the modeling by considering an additional state for the cells, namely, "burned-out" state.

- As pointed out in FireSmart [16], in risk assessment and management of WIIs (with an emphasis on oil and gas industry), both the threat of wildfire to industrial plants (risk) and the threat of industrial plants to the wildland (liability) should be considered. Regarding the liability, the capability of industry-caused fires in igniting forest vegetation and causing wildfires should be assessed and reduced. In the present study, however, we considered only the impact of wildfire on the oil facility (risk), overlooking the capability of burning tanks in igniting their adjacent cells (liability).

5. Conclusions

Extensive development of wildland-industrial interfaces (WIIs) from one side and global warming and an anticipated increase in the frequency of consequent wildfires from the other hand demand for modeling and risk assessment of wildfires in WIIs. In particular, if a WII is characterized by large inventory of hazardous chemicals, the consequences of wildfires could worsen due to the possibility of triggering secondary fires and explosions.

In the present study, we developed a fire spread model to predict the growth and spread of fire in WIIs, both in the wildland and in the industrial area. To this end, the WII was first modeled as a lattice and then mapped into a dynamic Bayesian network (DBN). Considering wind as one of the most influential parameters in controlling the direction of fire spread, the Canadian Fire Behavior Prediction (FBP) system was employed to derive the fire's rate of spread and intensity, which in turn were used to calculate the conditional fire spread probabilities among the nodes of the DBN. Having the spread probabilities, the most probable path of fire and respective burn probabilities were identified by the DBN.

In developing the model, we made simplifying assumptions such as constant weather and fuel conditions, which in conjunction with the uncertainties embedded in the FBP system with regard to the prediction of fire's rate of spread and intensity, may reduce the accuracy of the burn probabilities. Such simplifications can be relaxed in future works by, for instance, increasing the resolution of the representative lattice (increasing the possibility of fuel heterogeneity within a cell), considering the wind direction and speed as random variables, and including the fire residence time in the analysis.

Knowing that perfect near-time predictions would never be achieved [10], the model predictions should only serve as a guide to help land use developers, firefighters, and plant owners get a better handle of the fire's most probable path and burn probabilities, and accordingly optimize their risk management strategies. In the absence of fire spread models in WIIs, the developed model, despite its limitations, is the first of its kind, and can provide a new direction in modeling and risk assessment of wildfires in WIIs.

References

[1] Goldammer J, Mitsopoulos I, Mallinis G, Woolf M. (2017). Wildfire Hazard and Risk Assessment. In: Words into Action Guidelines: National Disaster Risk Assessment. United Nations Office for Disaster Risk Reduction. Available at: https://www.unisdr.org/files/52828_nationaldisasterriskassessmentwiagu.pdf. Last checked on 22-10-2018.

[2] Romps DM, Seeley JT, Vollaro D, Molinari J. Projected increase in lightning strikes in the United States due to global warming. Science, 2014, 346(6211), 851-854.

[3] Flannigan MD, Wotton BM, Marshall GA, de Groot WJ, Johnston J, Jurko N, Cantin AS. Fuel moisture sensitivity to temperature and precipitation: climate change implications. Climatic Change, 2016, 134, 59–71.

[4] National Geographic. Learn more about wildfires. Available at: https://www.nationalgeographic.com/environment/natural-disasters/wildfires/. Last checked on 27-7-2018.

[5] FAO (2007) Fire management global assessment 2006. A thematic study prepared in the framework of the Global Forest Resources Assessment 2005. UN Food and Agriculture Organization, Forest Management Division, Forest Paper 151. (Rome, Italy) Available at: http://www.fao.org/docrep/009/a0969e/a0969e00.htm. Last checked on 11-11-2018.

[6] Johnston LM, Flannigan MD. Mapping Canadian wildland fire interface areas. International Journal of Wildland Fire, 2018, 24, 1-14.

[7] Preisler HK, Brillinger DR, Burgan RE, Benoit JW. Probability based models for estimation of wildfire risk. International Journal of Wildland Fire, 2004, 13(2), 133-42.

[8] Scott J, Helmbrecht D, Thompson MP, Calkin DE, Marcille K. Probabilistic assessment of wildfire hazard and municipal watershed exposure. Natural Hazards, 2012, 64,707–728.

[9] Scott J, Thompson MP, Calkin DE. 2013. A wildfire risk assessment framework for land and resource management. General Technical Report RMRS-GTR-315. U.S. Department of Agriculture, Forest Service, Rocky Mountain Research Station. 83 p.

[10] Alexandre ME, Cruz MG. Limitations on the accuracy of model predictions of wildland fire behavior: A state-of-the-knowledge overview. The Forestry Chronicle, 2013, 89(3), 370-381.

[11] Khakzad N, Dadashzadeh M, Reniers G. Quantitative assessment of wildfire risk in oil facilities. Journal of Environmental Management, 2018, 223, 433-443.

[12] Khakzad N. Impact of wildfires on Canada's oil sands facilities. Natural Hazards and Earth System Sciences, 2018, 18: 3153-3166.

[13] Mining.Com (2015). Wildfire spreads closer to Canada's oil sands: hundreds evacuated. May 28, 2015. Available from: http://www.mining.com/wildfire-spreads-closer-to-canadas-oil-sands-hundreds-evacuated/. Last checked on 27-7-2018.

[14] Maclean's (2016). The Fort McMurray wildfire has hit the oil sands hard. May 6, 2016. Available from: http://www.macleans.ca/economy/the-fort-mcmurray-wildfire-has-hit-the-oil-sands-hard/. Last checked on 27-7-2018.

[15] https://globalnews.ca/news/2706177/fort-mcmurray-wildfire-several-homes-damaged-in-explosion- in-dickinsfield-fire-in-thickwood/

[16] FireSmart®. 2012. Canadian Guidebook for the Oil and Gas Industry. Alberta, Canada. Available from: http://wildfire.alberta.ca/firesmart/documents/FireSmart-Guidebook-OilAndGasIndustry-2008.pdf

[17] Heymes F, Aprin L, Forestier S, Slangen P, Jarry JB, François H, Dusserre G. Impact of a distant wildland fire on an LPG tank, Fire Safety Journal, 2013, 61, 100–107.

[18] Forestry Canada Fire Danger Group. 1992. Development and structure of the Canadian Forest Fire Behavior Prediction System. For. Can. Ottawa, ON. Inf. Rep. ST-X-3. Available at: http://cfs.nrcan.gc.ca/pubwarehouse/pdfs/10068.pdf. Last checked 13-11-2018.

[19] Khakzad N. Application of dynamic Bayesian network to risk analysis of domino effects in chemical infrastructures. Reliability Engineering & System Safety, 2015, 138, 263-272.

[20] Albini FA. 1984. Wildland fires. American Scientist, 72: 590–597.

[21] Finney MA. The challenge of quantitative risk analysis for wildland fire. Forest Ecology and Management, 2005, 211, 97–108.

[22] Miller C, Ager AA. A review of recent advances in risk analysis for wildfire management. International Journal of Wildland Fire, 2013, 22, 1-14.

[23] Chuvieco E, Aguado I, Dimitrakopoulos AP. Conversion of fuel moisture content values to ignition potential for integrated fire danger assessment. Canadian Journal of Forest Research, 2004, 34(11), 2284-2293.

[24] Larjavaara M, Kuuluvainen T, Tanskanen H, Venäläinen A. Variation in forest fire ignition probability in Finland, Silva Fennica, 38(3), 253-266, 2004.

[25] Jurdao S, Chuvieco E, Jorge M, Arevalillo JM. Modelling fire ignition probability from satellite estimates of live fuel moisture content. Fire Ecology, 2012, 8(1), 77-97.

[26] Rorig Ml, Ferguson SA. Characteristics of Lightning and Wildland Fire Ignition in the Pacific Northwest. Journal of Applied Meteorology, 1999, 38, 1565-1575.

[27] Anderson KR. A model to predict lightning-caused fire occurrences. Int. J. Wildland Fire, 2002, 11, 174–182.

[28] Lawson BD, Armitage OB, Dalrymple GN. 1994. Ignition probabilities for simulated people-caused fires in B.C.'s lodge pole pine and white spruce-subalpine fir forests. Pages 493–505, 12th Conference on Fire and Forest Meteorology. Oct. 26–28, 1993, Jekyll Isl. GA. Soc. Am. For. Bethesda, MD.

[29] Miller C, Parisien MA, Ager AA, Finney MA (2008) Evaluating spatially explicit burn probabilities for strategic fire management planning. In: Modelling, Monitoring, and Management of Forest Fires, Editors: J De las Heras, CA Brebbia, D Viegas, V Leone, pp. 245–252, WIT Press: Boston, MA.

[30] Syphard AD, Radeloff VC, Keely JE, Hawbaker TJ, Clayton MK, Stewart SI, Hammer RB. Human influence on California fire regimes. Ecological Applications, 2007, 17, 1388–1402.

[31] Byram GM. 1959. Combustion of forest fuels. In: Forest fire: control and use, 2nd edition. New York: McGraw-Hill: 61–89.

[32] Rothermel RC. 1972. A mathematical model for predicting fire spread in wildland fuels. Res. Pap. INT-115. Ogden, UT: U.S. Department of Agriculture, Forest Service, Intermountain Forest and Range Experiment Station. 40 p.

[33] Thomas PH. 1963. The size of flames from natural fires. In: Proceedings of the ninth symposium on combustion; 1962. New York: Academic Press: 844–859.

[34] van Wagner CE. Conditions for the start and spread of crown fire. Canadian Journal of Forest Research, 1977, 7(1), 23-34.

[35] Rothermel RC. 1991. Predicting behavior and size of crown fires in the Northern Rocky Mountains. Res. Pap. INT-438. Ogden, UT: U.S. Department of Agriculture, Forest Service, Intermountain Forest and Range Experiment Station. 46 p.

[36] Albini FA. Spot fire distance from burning trees-a predictive model. Tech. Rep. Gen. Tech. Rep. INT-56, U.S. Department of Agriculture, Forest Service, Intermountain Forest and Range Experiment Station, Ogden, UT, USA (1979).

[37] Koo E, Pagni PJ, Weise DR, Woycheese JP. Firebrands and spotting ignition in large-scale fires. International Journal of Wildfire, 2010, 19,818-843.

[38] Bak P, Chen K, Tang C. A forest-fire model and some thoughts on turbulence. Physics Letters A, 1990, 147(5,6), 297-300.

[39] Chen K, Bak P, Jensen MH. A deterministic critical forest fire model. Physics Letters A, 1990, 149(4), 207-210.

[40] Drossel B, Schwabl F. Self-organized critical forest-fire model. Physical Review Letters, 1992, 69(11), 1629-1632.

[41] Finney MA. Fire growth using minimum travel time methods. Canadian Journal of Forest Research, 2002, 32, 1420-1424.

[42] Roloff GJ, Mealey SP, Clay C, Barry J, Yanish C, Neuenschwander L. (2005). A process for modeling short- and long-term risk in the southern Oregon Cascades. Forest Ecology and Management 211, 166–190.

[43] Carmel Y, Paz S, Jahashan F, Shoshany M (2009) Assessing fire risk using Monte Carlo simulations of fire spread. Forest Ecology and Management 257, 370–377.

[44] Stepanov A, Smith JM. Modeling wildfire propagation with delaunay triangulation and shortest path algorithms. European Journal of Operational Research, 2012, 218,775-788.

[45] Mraz M, Zimic N, Virant J. Intelligent bush fire spread prediction using fuzzy cellular automata. Journal of Intelligent & Fuzzy Systems, 1999, 7, 203-207.

[46] Karafyllidis I. Design of a dedicated parallel processor for the prediction of forest fire spreading using cellular automata and genetic algorithms. Engineering Applications of Artificial Intelligence, 2004, 17, 19-36.

[47] Boychuk, D, Braun WJ, Kulperger RJ, Krougly ZL, Stanford DA. 2009. A stochastic forest fire growth model. Environmental and Ecological Statistics, 16(2), 133-151.

[48] Hajian M, Melachrinoudis E, Kubat P. Modeling wildfire propagation with the stochastic shortest path: A fast simulation approach. Environmental Modelling & Software, 2016, 82, 73-88.

[49] Mahmoud H, Chulahwat A. Unraveling the complexity of wildland urban interface fires. Scientific Reports, 2018, 8: 9315, 1-12.

[50] Andrews P. (1986). BEHAVE : Fire behavior prediction and fuel modeling system - BURN subsystem, part 1. USDA Forest Service, Intermountain Forest and Range Experiment Station, General Technical Report INT-194, 130 pp. Available from: https://digitalcommons.usu.edu/cgi/viewcontent.cgi?referer=https://www.google.nl/&httpsredir=1&article=1148&context=barkbeetles. Last checked on 22-10-2018.

[51] Knight I, Coleman J. A fire perimeter expansion algorithm based on huygens' wavelet propagation. International Journal of Wildland Fire, 1993, 3, 73–84.

[52] Finney MA. FARSITE: fire area simulator–model development and evaluation. Tech. Rep. RMRS-RP-4, U.S. Department of Agriculture, Forest Service, Rocky Mountain Forest and Range Experiment Station, Ogden, Utah, USA (1998).

[53] Papadopoulos GD, Pavlidou FN. A comparative review on wildfire simulators. IEEE Systems Journal, 2011, 5(2), 233-243.

[54] Scott JH. NEXUS: a system for assessing crown fire hazard. Fire Management Notes, 1999, 59(2), 21–24.

[55] Finney MA. An overview of FlamMap fire modeling capabilities. USDA Forest Service Proceedings RMRS-P-41. 2006, 213-220. Available from: https://www.fs.usda.gov/treesearch/pubs/25948. Last checked on 21-10-2018.

[56] Andrews P. BehavePlus fire modeling system: Past, present, and future. Proceedings of 7th Symposium on Fire and Forest Meteorology; 23-25 October 2007, Bar Harbor, Maine. Boston, MA: American Meteorological Society. 13 p. Available from:

https://www.fs.usda.gov/treesearch/pubs/31549. Last checked on 22-10-2018.

[57] Reinhardt ED, Dickinson MB. First-order fire effects models for land management: Overview and issues. Fire Ecology, 2010, 6(1), 131–142.

[58] Finney MA, Grenfell IC, McHugh CW. A method for ensemble wildland fire simulation. Environmental Modeling and Assessment, 2010, 16, 153–167.

[59] Catchpole EA, de Mestre NJ, Gill AM. Intensity of fire at its perimeter. Australian Forest Research, 1982, 12, 47-54.

[60] Alexander ME, Cruz MG. Interdependencies between flame length and fireline intensity in predicting crown fire initiation and crown scorch height. International Journal of Wildland Fire, 2012, 21, 95–113.

[61] Alexander M. Forest Health: fire behavior considerations. Post-Harvest Stand Development Conference, Edmonton, Canada, 31 January – 1 February, 2006. Available from: https://fgrow.friresearch.ca/sites/default/files/null/FGYA_2006_02_Prsnttn_PostHarvestStandDevConference_ForestHealthFireBehaviourConsiderations.pdf. Last checked on 2-11-2018.

[62] Alexander ME. Calculating and interpreting forest fire intensities. Canadian Journal of Botany, 1982, 60(4), 349-357.

[63] Cozzani V, Gubinelli G, Antonioni G, Spadoni G, Zanelli S. The assessment of risk caused by domino effect in quantitative area risk analysis. Journal of Hazardous Materials, 2005, A127, 14–30.

[64] Landucci G, Gubinelli G, Antonioni G, Cozzani V. The assessment of the damage probability of storage tanks in domino events triggered by fire. Accident Analysis and Prevention, 2009; 41: 1206–1215.

[65] Butler BW, Cohen JD. Field verification of a firefighter safety zone model. Proceedings of the 2000 International Wildfire Safety Summit, Edmonton, Alberta, October 10-12, 2000, pp: 54-61.

[66] Zárate L, Arnaldos J, Casal J. Establishing safety distances for wildland fires. Fire Safety Journal, 2008, 43, 565–575.

[67] Moudan KS. Geometric view factors for thermal radiation hazard assessment. Fire Safety Journal, 1987, 12, 89-96.

[68] Assael MJ, Kakosimos KE. Fires, explosions, and toxic gas dispersions: effects calculation and risk analysis. 2010, CRC Press, Taylor & Francis Group, Boca Raton, FL.

[69] Pearl J. Probabilistic Reasoning in Intelligent Systems. San Francisco, CA: Morgan Kaufmann, 1988.

[70] Dechter R. Bucket elimination: A unifying framework for probabilistic inference. In Proceedings of the Conference on Uncertainty in Artificial Intelligence. Morgan Kaufmann, San Francisco, 1996, pp. 211–219.

[71] Lauritzen SL, Spiegelhalter DJ. Local computations with probabilities on graphical structures and their application to expert systems. Journal of Royal Statistical Society, 1988; 50: 157-224.

[72] Jensen F. An Introduction to Bayesian Networks. UCL Press, Springer-Verlag Berlin, Heidelberg 1996.

[73] Pearl J. Reverend Bayes on inference engines: A distributed hierarchical approach. Proceedings of the Second National Conference on Artificial Intelligence. AAAI-82: Pittsburgh, PA. Menlo Park, California, 1982: AAAI Press. pp. 133–136.

[74] Cheng J, Druzdzel MJ. Computational investigation of low-discrepancy sequences in simulation algorithms for Bayesian networks. In Proceedings of the 16th Conference on Uncertainty in Artificial Intelligence, Morgan Kaufmann (1999), 72–81.

[75] Khakzad N, Khan F, Amyotte P, Cozzani V. Domino effect analysis using Bayesian networks. Risk Analysis, 2013; 33: 292–306.

[76] Wei Y, Rideout D, Kirsch A. An optimization model for locating fuel treatments across a landscape to reduce expected fire losses. Canadian Journal of Forest Research, 2008, 38, 868–877.

[77] Cruz MG, Sullivan AL, Gould JS, Sims NC, Bannister AJ, Hollis JJ, Hurley R. Anatomy of a catastrophic wildfire: The Black Saturday Kilmore East fire. Forest Ecology and Management, 2012, 284, 269-285.

[78] GeNIe Version 2.2 Academic Installer, Feb. 2018. Decision Systems Laboratory, University of Pittsburg, available online at: https://download.bayesfusion.com/files.html?category=Academia, Last checked 12-11-2018.

[79] ALOHA Version 5.4.7, September 2016, US Environmental Protection Agency, National oceanic and atmospheric administration, available at: https://www.epa.gov/cameo/aloha-software. Last accessed 12-11-2018.

[80] Cheney P, Sullivan A. Grassfires: Fuel, weather and fire behavior. 2nd edition. CSIRO Publ, Collingwood, VIC, 150 p, 2008.

Appendix

Identification of view factor in Solid Flame Model.

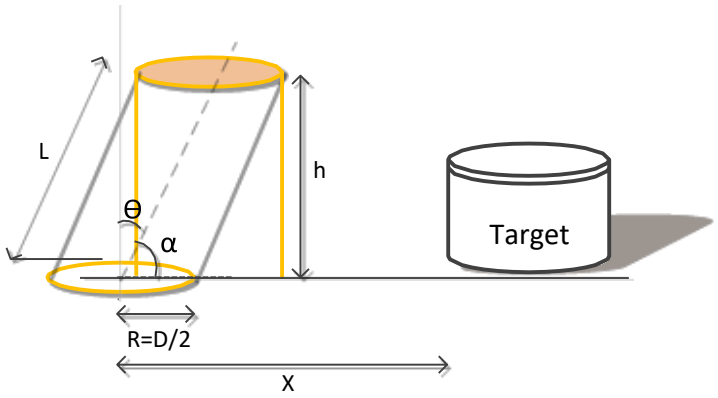

Figure A1. Considering the flame as a tilted cylinder in the Solid Flame Model.

F_{view} can be calculated as a function of vertical F_1 and horizontal F_2 view factors as [68]:

$$\sqrt{\qquad} \tag{A1}$$

where:

$$* \quad (\quad) \quad (\quad) + \qquad (—) \quad —— * \qquad (\qquad\qquad) \qquad (\quad ——) + \tag{A2}$$

$$(–) \quad —— * \qquad (\qquad\qquad) \qquad (\quad ——) + \quad * \quad (\quad) \quad (\qquad\qquad) + \qquad (—) \tag{A3}$$

$$– \tag{A4}$$

$$– \tag{A5}$$

$$– \tag{A6}$$

$$\sqrt{\qquad\qquad\qquad\qquad\qquad\qquad} \quad (\qquad) \qquad (\qquad) \tag{A7}$$

$$\sqrt{\qquad\qquad\qquad\qquad\qquad\qquad} \quad (\qquad) \qquad (\qquad) \tag{A8}$$

√ ( ) (A9)

√( ) ( ) (A10)

——— (A11)

√——— (A12)

θ can be calculated as a function of wind speed u_w as:

—— (A13)

where Fr is the Froud number , and ~~Re is~~ the Reynolds number.

and are, respectively, the density (~ 1.21 kg/m^3) and viscosity (~ 16.7 μ.Pa.s) of air; g is gravitational acceleration (~ 9.81 m/s^2).

Graphical Abstract